



RANS Simulation of Turbulent Diffusive Combustion using Open Foam

L. F. Gutiérrez^{1,2†}, José P. Tamagno¹ and Sergio A. Elaskar^{1,2}

¹ *Departamento de Aeronáutica, Universidad Nacional de Córdoba, Córdoba, 5000, Argentina*

² *Consejo Nacional de Investigaciones Científicas y Técnicas -CONICET, Argentina*

† *Corresponding Author Email: lfgmarcantoni@gmail.com*

(Received October 16, 2014; accepted February 24, 2015)

ABSTRACT

Schemes to write the flow equations in discrete form, solution solvers, pre and post data processing utilities provided by OpenFoam libraries, are used to build a finite volume executable for simulating a low speed, turbulent and rate controlled diffusive CH₄-Air combustion. Unsteady Favre's averaged turbulent conservation equations (total mass, momentum, energy and species mass fractions), are used to describe the combustion gas dynamics, and to handle turbulence a modified *k-ε* model is applied. Several global kinetic mechanisms, one step, two and four steps have been considered to describe the oxidation process of CH₄ in a free jet type flame. The interaction between chemistry and turbulence, is modeled according to the partially stirred reactor (PaSR) concept. To improve convergence and accuracy in solving low speed fluid dynamic equations, a pressure implicit with splitting of operators (PISO) technique extended to cover high temperature flows, is utilized. The exponential dependence of the chemical kinetics from temperature, makes stiff the ODE's needed to determine source average values with which the species conservation equations are solved. To deal with the stiffness issue, OpenFoam provides numerical schemes that guarantee the stability of the computation. Comparisons between results of numerical simulations and experimental data obtained with the benchmark known as flame "D", are presented.

Keywords: Numerical simulation; Turbulent diffusive combustion; Global reaction; Flame D.

NOMENCLATURE

A_0	pre-exponential factor	Δt	time step
\bar{D}_k	mean species molecular diffusion coefficient	ϵ	turbulent kinetic energy dissipation
h_s	sensible enthalpy	κ	volume reactive fraction
k	turbulent kinetic energy	λ	thermal conductivity coefficient
p	pressure	μ	molecular viscosity coefficient
Pr_l	Prandtl number	μ_t	turbulent viscosity coefficient
RR	reaction rate	μ_{eff}	effective viscosity coefficient
T	temperature	ρ	density
T_a	activation temperature	τ_{ij}	viscous stress tensor
r	pilot inlet radius	τ_{ch}	chemical time
u	velocity	τ_{mix}	mixing time
V_k	diffusion velocity of specie k	$\bar{\omega}_k$	production/consumption rate of specie k
Y_k	mass fraction of specie k	$\bar{\omega}_T$	heat released by combustion
W_k	molecular weight of specie k	\sim	Favre averaged quantity
\mathcal{V}_p	control volume	$-$	Reynolds averaged quantity

1. INTRODUCTION

openFoam (Open Field Operation and Manipulation Weller *et al.* (1998)), can be seen like a

big toolbox that provides libraries and applications to meet nearly all tasks involved on main steps of finite volume CFD simulations. Islam *et al.* (2009), Singh *et al.* (2011), Filho

et al. (2011), have show the utilization of OpenFoam to treat incompressible aerodynamic problems. Turbo machinery applications have been reported by Beaudoin and Jasak (2008), Mangani (2008), Muntean *et al.* (2009) and Benajes *et al.* (2014). Diesel engine combustion modeling, including spray simulation are presented by Nordin (2001), Kärrholm *et al.* (2008) and Novella *et al.* (2011). Marzouk and Huckaby (2010), have made studies of chemical kinetics models related to syngas burning.

Here are presented results for the piloted free jet flame D, a benchmark case carefully studied experimentally in the Combustion Research Facility of Sandia National Laboratories (USA). The available experimental data covers the period 1998-2007 Barlow and Frank (1998), Barlow and Frank (2007). Nooren *et al.* (2000) made contributions on subjects related to turbulence effects in CH₄-air jet flames and on measurements techniques. Temperature and species mass fractions measurements have been conducted using Raman-Rayleigh scattering techniques. It prevents possible inconsistencies in comparing Favre averaged predictions with Reynolds averaged measurements. In addition, the flame D has a small probability of local extinction Barlow and Frank (2007), becoming suitable for comparisons with models not including a flame extinction criteria.

When finite rate chemistry processes are considered, a decision has to be made about kinetic mechanisms to be used, since it could have a great impact on computing times. In line with the main purpose of this work, gaining experience on the use of openFoam to build executable solvers and testing its usefulness to study turbulent diffusive combustion, simplified reaction mechanisms for the oxidation of CH₄ fuel have been examined. The types of mechanisms studied include one reaction step Bui-Pham (1992), two reaction steps (Westbrook and Dryer (1981)), with Andersen *et al.* (2009) rates, and the Wang *et al.* (2012) modification adding a H₂ oxidation reaction, and four reaction steps proposed by Jones and Lindstedt (1988) where reverse parameters used in CO and H₂ oxidation's, are now calculated using equilibrium constants Wang *et al.* (2012). Two and four steps mechanisms were programed for use with openFoam. In each cell of the computational domain and for every flow time step, the calculation of each species source term requires the integration of ordinary differential equations (ODE's). However, these ODE's are stiff and to guaranty stability the semi implicit numerical method of Bader and Deuffhard (1983) (SIBS)

included in the OpenFoam solvers library, has been selected.

The flame D develops in a low speed environment, however due to strong temperature changes associated with chemical heat release ($300 \leq T < 2500$ K), compressible effects arise. When the Mach number goes to zero, the compressible governing equations should in a continuous sense, approach their incompressible counterpart and density tends to become independent of pressure. Then, the continuity equation is no suitable to compute the density as a dependent variable wherein the pressure is evaluated from it via an equation of state. To handle these issues, methods based on solving a new transport equation for pressure is formulated. Here the pressure-velocity coupling solution method known as PISO (for pressure implicit with splitting of operators) applicable to compressible flow is employed (Issa (1986), Benajes *et al.* (2014)). Further details about the PISO method are given in the section where fundamental aspects of numerical techniques are treated.

All openFoam codes are built for a three dimensional (3D) space and all meshes have to be defined in a 3D manner. However, the shape of the computational domain in which the simulations are carried out is axial symmetric. In OpenFoam, an axial symmetric wedge shaped geometry can be generated by defining first a 3D mesh, and thereafter specifying front and back sides of the axial symmetric domain as wedge patches where appropriate boundary conditions are applied. Details for generating axial symmetric wedge shaped geometries using blockMesh (utility for generating simple meshes with blocks of hexahedral cells) and employing wedge patch from libfiniteVolume library can be found on the openFoam user guide OpenCFD (2009)¹.

It is assumed that the Navier-Stokes equations are to a multi-species reacting gas also applicable, and that conservation equations (continuity, momentum, species and energy) in RANS simulations can be written in terms of mass weighted Favre averages Favre (1969). With this formalism, the averaged balance equations become Poinot and Veynante (2005):

Global mass

$$\frac{\partial \bar{\rho}}{\partial t} + \frac{\partial}{\partial x_i} (\bar{\rho} \tilde{u}_i) = 0 \quad (1)$$

¹The wedge patches technique has been successfully applied in computing supersonic-hypersonic flows around axisymmetric blunt bodies Gutiérrez *et al.* (2012)

Momentum

$$\frac{\partial}{\partial t} (\bar{\rho} \tilde{u}_j) + \frac{\partial}{\partial x_i} (\bar{\rho} \tilde{u}_i \tilde{u}_j) + \frac{\partial \bar{p}}{\partial x_j} = \frac{\partial}{\partial x_i} (\overline{\tau_{i,j}} - \bar{\rho} \tilde{u}_i \tilde{u}_j) \quad (2)$$

Chemical species (for $k = 1, N$)

$$\frac{\partial}{\partial t} (\bar{\rho} \tilde{Y}_k) + \frac{\partial}{\partial x_i} (\bar{\rho} \tilde{u}_i \tilde{Y}_k) = - \frac{\partial}{\partial x_i} (\overline{V_{k,i} Y_k} + \bar{\rho} \tilde{u}_i \tilde{Y}_k) + \bar{\omega}_k \quad (3)$$

Energy equation in terms of the mixture sensible enthalpy

$$\frac{\partial}{\partial t} (\bar{\rho} \tilde{h}_s) + \frac{\partial}{\partial t} (\bar{\rho} \tilde{u}_i \tilde{h}_s) = \bar{\omega}_T + \frac{\overline{Dp}}{Dt} + \frac{\partial}{\partial x_i} \left(\overline{\lambda \frac{\partial T}{\partial x_i}} - \bar{\rho} \tilde{u}_i \tilde{h}_s \right) + \overline{\tau_{i,j} \frac{\partial u_i}{\partial x_j}} - \frac{\partial}{\partial x_i} \left(\overline{\rho \sum_{k=1}^N V_{k,i} Y_k h_{s,k}} \right) \quad (4)$$

where

$$\frac{\overline{Dp}}{Dt} = \frac{\partial \bar{p}}{\partial t} + \tilde{u}_i \frac{\partial \bar{p}}{\partial x_i} \quad (5)$$

Note that these equations are formally identical to the classic Reynolds averaged equations for constant density flows.

2. UNCLOSED TERMS IN FAVRE AVERAGED BALANCE EQUATIONS

In what follows, closures for the unknown quantities found in Eq. 1 to Eq. 5 are proposed.

2.1 Reynolds Stresses ($\tilde{u}_i \tilde{u}_j$)

Following the assumption proposed by Boussinesq Wilcox (1998), modeling of turbulent Reynolds stresses require the prior assesment of the turbulence dynamic viscosity μ_t . A two equations turbulence model Jones and Launder (1972), Nordin (2001), Kärholm (2008) that will provide values for the flow turbulent kinetic energy \tilde{k} and for its dissipation $\tilde{\epsilon}$ is used to estimate the turbulent viscosity as

$$\mu_t = C_\mu \bar{\rho} \frac{\tilde{k}^2}{\tilde{\epsilon}} \quad (6)$$

where C_μ (usually given the value 0.09), is one of the many coefficients needed to close the two equations turbulence model. These two equations are PDE's that must be solved with the conservation equations simultaneously.

2.2 Species ($\tilde{u}_i \tilde{Y}_k$) and Enthalpy ($\tilde{u}_i \tilde{h}_s$) Turbulent and Laminar Fluxes

Species laminar diffusion fluxes can be modeled as

$$\bar{\rho} \overline{V_{k,i} Y_k} \approx -\bar{\rho} \bar{D} \frac{\partial \tilde{Y}_k}{\partial x_i} \quad (7)$$

on conditions that molecular diffusion follows the Fick's law and the molecular diffusivity of species D_k are assumed equals ($D_k = \bar{D}$). If in addition, the transport due to molecular diffusion of species is assumed comparable to the rate of transport due to viscous effects, then $\bar{\rho} \bar{D} \equiv \mu_l$, Chung (2006). The mixture dynamic molecular viscosity is now denoted by μ_l .

If species turbulent diffusion fluxes are also closed using a gradient approach (Kuo (2005), Chung (2006), Lilleberg *et al.* (2013)), and turbulent diffusion transport is again assumed comparable to the rate of transport due to turbulent viscous effects Bird *et al.* (2007) then

$$\bar{\rho} \tilde{u}_i \tilde{Y}_k \approx -\mu_t \frac{\partial \tilde{Y}_k}{\partial x_i} \quad (8)$$

where μ_t is the turbulent viscosity. By adding both laminar and turbulent diffusion fluxes, the corresponding terms in the species conservation equation (Eq. 3) can be written

$$\frac{\partial}{\partial x_i} \left(\bar{\rho} \overline{V_{k,i} Y_k} + \bar{\rho} \tilde{u}_i \tilde{Y}_k \right) \approx -(\mu_l + \mu_t) \frac{\partial \tilde{Y}_k}{\partial x_i} = -\mu_{eff} \frac{\partial \tilde{Y}_k}{\partial x_i} \quad (9)$$

where μ_{eff} is an averaged dynamic viscosity of the reaction mixture.

The laminar heat diffusion expressed by Fourier law can be written as

$$\overline{\lambda \frac{\partial T}{\partial x_i}} \approx \bar{\lambda} \frac{\partial T}{\partial x_i} \approx \frac{\bar{\lambda}}{C_p} \frac{\partial \tilde{h}_s}{\partial x_i} = \frac{\mu}{Pr_l} \frac{\partial \tilde{h}_s}{\partial x_i} \quad (10)$$

where $\bar{\lambda}$ denotes a local mean molecular thermal diffusivity and $\bar{C}_p = \sum_k^N Y_k C_{p,k}(T)$ a local mean specific heat. $C_{p,k}(T)$ and $h_{s,k}(T)$ are computed using JANAF Tables Stull and Prophet (1971).

The unclosed term $\bar{\rho} \tilde{u}_i \tilde{h}_s$ is by analogy with the laminar case modeled as:

$$\bar{\rho} \tilde{u}_i \tilde{h}_s = -\frac{\mu_t}{Pr_t} \frac{\partial \tilde{h}_s}{\partial x_i} \quad (11)$$

Viscous heating, $\overline{\tau_{i,j} \frac{\partial u_i}{\partial x_j}}$ (Eq. 4), are neglected in the energy equation.

3. TURBULENCE-CHEMISTRY INTERACTION MODEL

The turbulence-chemistry interaction is modeled based on the partially stirred reactor (PaSR) approach where each computational cell is divided into two zones: a reacting zone, modeled as a perfectly stirred reactor (PSR) and a non reacting zone. A volume reactive fraction κ function of the computational time step Δt and time scales related with chemical (τ_{ch}) and mixing (τ_{mix}) processes, has been proposed Marzouk and Huckaby (2010):

$$\kappa = \frac{\Delta t + \tau_{ch}}{\Delta t + \tau_{ch} + \tau_{mix}} \quad (12)$$

Note that if $\tau_{ch} \rightarrow \infty$; $\kappa \rightarrow 1$, and if $\tau_{mix} \rightarrow \infty$; $\kappa \rightarrow 0$.

The τ_{mix} time is computed according to

$$\tau_{mix} = C_{mix} \sqrt{\frac{\mu_{eff}}{\rho \bar{\epsilon}}} \quad (13)$$

The value given to constant C_{mix} is taken as 0.3 Nordin (2001).

Conversion rates of fuel, or oxygen are used to define the characteristic chemical time τ_{ch} through the expression

$$\frac{1}{\tau_{ch}} = \max \left(\frac{-\tilde{\omega}_{Fuel}}{\bar{\rho}}, \frac{-\tilde{\omega}_{O_2}}{\bar{\rho}} \right) \quad (14)$$

The rate of change of the mean species mass concentrations $\bar{\omega}_k$ can then, be calculated by

$$\bar{\omega}_k = \kappa W_k \sum_{i=1}^M \left(\frac{dC_k}{dt} \right)_i \quad (15)$$

being M the number of reactions, W_k the molecular weight of species k and $\left(\frac{dC_k}{dt} \right)_i$ the rate of formation of species C_k from reaction i . Eq. 14 computes de average source term for the species k conservation equation.

The total heat $\bar{\omega}_T$ released by the combustion is computed according to

$$\bar{\omega}_T = \sum_{k=1}^N \bar{\omega}_k \Delta h_{f,k}^0 \quad (16)$$

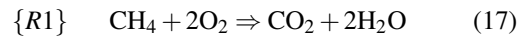
being N the number of species, $\Delta h_{f,k}^0$ the formation enthalpy of species k .

4. REACTION MECHANISMS FOR THE OXIDATION OF METHANE IN FLAMES

Four simplified reaction mechanisms for the oxidation of CH_4 to be evaluated for a well documented piloted flame “D”, are proposed.

The Bui Pham one step mechanism (BP)

A single forward global reaction applicable to the methane oxidation process is considered Bui-Pham (1992):



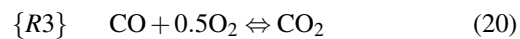
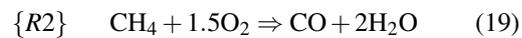
The one step reaction is often a convenient way of approximating the effects of the many reactions which actually occur. The rate expression of the single reaction is expressed in terms of the Arrhenius law and therefore written as

$$\begin{aligned} RR_1 &= A T^\beta \exp \left(-\frac{E_a}{R_u T} \right) [Fuel]^a [Oxidizer]^b \\ &= A T^\beta \exp \left(-\frac{E_a}{R_u T} \right) [CH_4]^a [O_2]^b \end{aligned} \quad (18)$$

A is the pre-exponential factor, β the temperature exponent, E_a the activation energy, R_u the universal gas constant. The ratio E_a/R_u is called the activation temperature. Observe that the exponent a and b may not be stoichiometric values.

The Westbrook and Dryer two steps mechanism (WD)

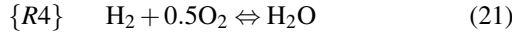
The reaction mechanism for Westbrook and Dryer (1981) model are:



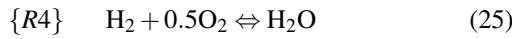
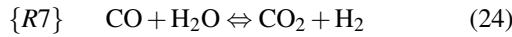
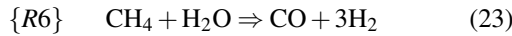
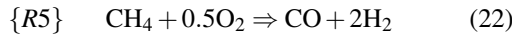
To account at least in part for the effects of incomplete conversion to CO_2 and H_2O , and to include qualitatively the sequential nature of the process of hydrocarbon oxidation, Westbrook and Dryer (1981) develop a two steps reaction mechanism, being the last step a reversible oxidation of CO to CO_2 . The rate constants for $\{R2\}$ and $\{R3\}$ originated from their studies for CH_4 and CO oxidation reactions in a turbulent reactor. However, the original rate coefficients for the $\{R3\}$ reaction, were modified to secure an approach to equilibrium values for CO and CO_2 Andersen *et al.* (2009).

The modified mechanism of Westbrook and Dryer (WDM)

The initial volume fraction of CO₂ influence the process of CO oxidation, but the presence of H₂O acting as a sort of third body can also affect the CO oxidation. Wang *et al.* (2012), modified the Westbrook and Dryer two steps mechanism by adding a H₂ oxidation rate expressed by the additional reaction:



The Jones and Lindstedt four steps mechanism (JL)



Jones and Lindstedt (1988), developed this four steps mechanism applicable to non premixed flames of hydrocarbons fuels. The rate {R5} is dominant in fuel lean mixtures and the rate {R6} is in fuel rich mixtures. The forward rate parameters of CO and H₂ oxidation's used in reactions {R7} and {R4}, have been proposed by Jones and Lindstedt (1988) and Marinov *et al.* (1996), respectively. The corresponding reverse parameters used in both oxidation reactions, are calculated by Wang *et al.* (2012), using tabulated equilibrium constants fitted by polynomials Kuo (2005).

Chemical kinetic data (Arrhenius parameters and reaction rate form) for each model used here are presented in Tab. 1.

5. FUNDAMENTAL ASPECTS OF THE NUMERICAL TECHNIQUES

Any unsteady transport equation for a scalar property ϕ is solved applying the Finite Volume (FV) method. The FV requires that any transport equation be satisfied over the control volume \mathcal{V}_P (Fig. 1) surrounding the point P in the integral form

$$\int_t^{t+\Delta t} \left[\frac{d}{dt} \int_{\mathcal{V}_P} \rho \phi d\mathcal{V} + \int_{\mathcal{V}_P} \nabla \cdot (\phi \rho U) d\mathcal{V} - \int_{\mathcal{V}_P} \nabla \cdot (\Gamma_\phi \nabla \phi) d\mathcal{V} \right] dt = \int_t^{t+\Delta t} \left[\int_{\mathcal{V}_P} S_\phi(\phi) d\mathcal{V} \right] dt \quad (26)$$

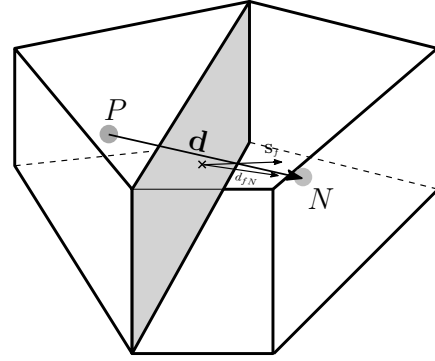


Fig. 1. Finite volume discretization.

The discretization of spatial convection term, diffusion term and source terms, can be split into two parts: the transformation of surface on volume integrals into discrete sums, and expression that give the face values of the variables as a functions of cells values. If also it is assumed that the control volumes do not change in time, E. 26. can be written Jasak (1996)

$$\int_t^{t+\Delta t} \left[\frac{d}{dt} (\rho \phi)_P + \sum_f F \phi_f - \sum_f (\rho \Gamma_\phi)_f \mathbf{S} \cdot (\nabla \phi)_f \right] dt = \int_t^{t+\Delta t} (S_u \mathcal{V}_P + S_p \mathcal{V}_P \phi_P) dt \quad (27)$$

Note that the source term has been linearized and that the volume integral is calculated as:

$$\int_{\mathcal{V}_P} S_\phi(\phi) dV = \int_{\mathcal{V}_P} (S_u + S_p \phi) dV = S_u \mathcal{V}_P + S_p \mathcal{V}_P \phi_P \quad (28)$$

Eq. 27 is usually call the semi-discretized form of the transport equation. Using the Euler implicit method for time discretization the final discrete form can be written:

$$\frac{1}{\Delta t} (\bar{\rho}^n \phi^n - \bar{\rho}^{n-1} \phi^{n-1}) \mathcal{V}_P + \sum_f F \phi_f^n - \sum_f (\rho \Gamma_\phi)_f \mathbf{S} \cdot (\nabla \phi^n)_f - S_u \mathcal{V}_P - S_p \mathcal{V}_P \phi_P^n = 0 \quad (29)$$

where $n - 1$ and n denotes successive time levels. Discrete equations for momentum and energy can be derived from Eq. 29 by replacing ϕ with \tilde{u} and \tilde{h}_s respectively ².

²Note that difussive terms need some special considerations

Table 1 Chemical Kinetics Information

Reaction	A	β	T_a	Rate	ref.
R1	5×10^{11}	0	14950	$[\text{CH}_4][\text{O}_2]$	Bui-Pham (1992)
R2	5.03×10^{11}	0	24056	$[\text{CH}_4]^{0.7}[\text{O}_2]^{0.8}$	Westbrook and Dryer (1981)
R3f	2.24×10^6	0	5032	$[\text{CO}][\text{O}_2]^{0.25}[\text{H}_2\text{O}]^{0.5}$	Andersen <i>et al.</i> (2009)
R3b	1.14×10^{13}	-0.97	39452	$[\text{CO}_2][\text{O}_2]^{-0.25}[\text{H}_2\text{O}]^{0.5}$	Andersen <i>et al.</i> (2009)
R4f	5.69×10^{11}	0	17609	$[\text{H}_2][\text{O}_2]^{0.5}$	Marinov <i>et al.</i> (1996)
R4b	2.51×10^{14}	0	47859	$[\text{H}_2\text{O}]$	Wang <i>et al.</i> (2012)
R4f-JL	7.91×10^{10}	0	17609	$[\text{H}_2][\text{O}_2]^{0.5}$	Marinov <i>et al.</i> (1996)
R4b-JL	3.48×10^{13}	0	47907	$[\text{H}_2\text{O}]$	Wang <i>et al.</i> (2012)
R5f	4.4×10^{11}	0	15095.7	$[\text{CH}_4]^{10.5}[\text{O}_2]^{1.25}$	Jones and Lindstedt (1988)
R6f	3×10^8	0	15095.7	$[\text{CH}_4][\text{H}_2\text{O}]$	Jones and Lindstedt (1988)
R7f	2.75×10^9	0	10063.8	$[\text{CO}][\text{H}_2\text{O}]$	Jones and Lindstedt (1988)
R7b	6.74×10^{10}	0	13688	$[\text{CO}_2][\text{H}_2]$	Wang <i>et al.</i> (2012)

It is said in the introduction that the pressure-velocity coupling solution algorithm PISO will be employed. Here the PISO method is outlined and its implementation described. Issa introduce a novel idea of PISO methodology Issa (1986), Jasak gives an appropriate description for the openFoam environment Jasak (2007), Jasak (1996). Starting from following semi-discrete form of the momentum equation:

$$a_P \tilde{U}_P^n = \mathbf{H}(\tilde{\mathbf{U}}) - \nabla \bar{p} \quad (30)$$

with

$$\mathbf{H}(\tilde{\mathbf{U}}) = \mathbf{R}_P - \sum a_N \tilde{U}_N^n \quad (31)$$

$$\text{and } \mathbf{R}_P = \mathbf{R}_0 + \frac{\mathbf{U}^{n-1}}{\Delta t}$$

and a_p are the center coefficients of the momentum equations. The discrete operator $\mathbf{H}(\tilde{\mathbf{U}})$ has two contributions: $(\sum a_N \tilde{U}_N^n)$ the contributions of all neighbors cells to cell P , \mathbf{R}_P a source contributions that contain the $(n-1)$ step of transient term $(\mathbf{U}^{n-1}(\Delta t)^{-1})$ and any other source contribution \mathbf{R}_0 (i.e, body forces).

The state equation is written $\rho = p\psi$, whereby the pressure temporal derivative can be obtained:

$$\frac{\partial \rho}{\partial t} = \frac{\partial}{\partial t}(p\psi) \quad (32)$$

By using Eq. 30, continuity (Eq. 1) and state equations the pressure equation (Eq. 33) is obtained:

$$\left(\frac{1}{\Delta t}\right) (p^n \psi^n - p^{n-1} \psi^{n-1}) V_P +$$

$$\nabla \cdot (\psi(a_P)^{-1} \mathbf{H}(\tilde{\mathbf{U}})_P) - \nabla \cdot (\rho(a_P)^{-1} \nabla p) = 0 \quad (33)$$

It should be noted that this equation has the standard form of Eq. 29 (rate of change, convective and diffusive terms), and discretization of any standard form equation can be handled in a stable, accurate and bounded manner Jasak (2007). Next it is showing how the PISO method is applied within the openFoam's environment and Fig. 2 shows corresponding flowchart.

1. Momentum equations are assembled and solved (first predictor step)³

```
fvVectorMatrix UEqn(
    fvm::ddt(rho, U) + fvm::div(phi, U)
    + turbulence->divDevRhoReff(U)
    == rho*g );
UEqn.relax();
if (momentumPredictor)
{solve(UEqn == -fvc::grad(p));}
```

2. Equations for mass fractions and enthalpy are assembled and solved. Thermophysical properties are corrected (i.e, compressibility is updated

$$\psi^* = \psi(T^*)$$

3. Pressure equation is assembled and solved (transonic flag is omitted) many times as PISO corrector steps (piso_{corr}) are performed :

```
1 rho = thermo.rho();
```

³ Note that turbulence is a pointer to the member function `divDevRhoReff` of the RANS turbulent models class. This member function returns $\mathbf{g}(\tilde{\mathbf{u}}) = \nabla \cdot (\mu_{\text{eff}} \nabla \tilde{\mathbf{u}}) - \nabla \cdot [\mu_{\text{eff}} \langle (\nabla \tilde{\mathbf{u}})^T - \frac{2}{3} I \text{tr} \{ (\nabla \tilde{\mathbf{u}})^T \} \}]$

```

2  volScalarField rUA = 1.0/UEqn.A();
3  U = rUA*UEqn.H();
4  {
5  phi = fvc::interpolate(rho)*
      ((fvc::interpolate(U) & mesh.Sf()));
6  + fvc::ddtPhiCorr(rUA, rho, U, phi));
7  for (int nonOrth=0;
      nonOrth<=nNonOrthCorr; nonOrth++){
8  fvScalarMatrix pEqn(
9  fvm::ddt(psi, p)+fvc::div(phi)
  - fvm::laplacian(rho*rUA, p)
10                                     );
11  pEqn.solve();
12  if (nonOrth == nNonOrthCorr){
13      phi += pEqn.flux();          }
14  }
15  }
16  #include "rhoEqn.H"
17  #include "compressibleContinuityErrs.H"

18  U -= rUA*fvc::grad(p);
19  U.correctBoundaryConditions();
20  DpDt = fvc::DDt(surfaceScalarField
("phiU", phi/fvc::interpolate(rho)), p);

```

At line 1 density is corrected ($\rho^n = \rho^{(n-1)}\psi^n$), a_p coefficients for momentum equations (line 2) and velocity (line 3) are updated employing the density obtained from first predictor step. Pressure flux is calculated (lines 5 and 6). Pressure equation is assembled from line 8 to 10:

$$fvm::ddt(psi, p) \rightarrow (p^n \psi^n - p^{n-1} \psi^{n-1}) V_P$$

$$fvc::div(phi) \rightarrow \nabla \cdot (\psi (a_p)^{-1} \mathbf{H}(U) p)$$

$$fvm::laplacian(rho*rUA, p)$$

$$\rightarrow \nabla \cdot (\rho (a_p)^{-1} \nabla p)$$

Here is important to note that the time advance is performed implicitly, the convective term is evaluated explicitly and the diffusive term implicitly. The namespaces `fvc` and `fvm` calculate explicit and implicit terms respectively (i.e. `fvc::grad(p)` evaluates ∇p by using data from last time step, and `fvm::laplacian(rho*rUA, p)` returns matrix coefficients of the discrete representation of $\nabla \cdot (\rho (a_p)^{-1} \nabla p)$). In consequence the pressure equation is solved implicitly at line 11 with the solution method selected at run time. If the orthogonal corrector steps imposed at run time are fulfilled, the flux are actualized (line 13). Then the continuity equation is solved and continuity errors are computed (lines 16-17). Velocity corrector step (momentum corrector) are performed (line 18):

$$U -= rUA*fvc::grad(p);$$

$$\rightarrow U_p^n = (a_p)^{-1} (\mathbf{H}(U) - \nabla p)$$

Boundary conditions for momentum equations are corrected (line 19). Finally the `volScalarField` associated with unsteady pressure term on the sensible enthalpy equation is actualized (line 20). The formal order of convergence of PISO technique depends on the corrector steps utilized, thus to obtain second order accuracy (in discretization errors) should at least two steps be performed Issa (1986).

Appropriate solution methods need to be selected to solve algebraic systems that come from discretization process. The solution algorithms can be selected as function of the system symmetry and convergence properties. For symmetric systems the pre-conjugate gradient method (PCG) with diagonal incomplete Cholesky preconditioner (DIC) is utilized because its rapid convergence properties Concus *et al.* (1985). In the other hand, convection/diffusion equation produces asymmetric matrices, for which bi-conjugate preconditioned method (BiPCG) with diagonal incomplete LU pre conditioner (DILU) has proved to be efficient Venkatakrishnan and Mavriplis (1993). For all solution algorithms a tolerance of 10^{-6} is fixed.

All equations time evolution is done by the Euler implicit scheme in conjunction with the stabilized local time stepping technique (SLTS) which allows solution advance in each cell with the maximum admissible time step, therefore convergence to steady state is accelerated Coquel *et al.* (2008), Blazek (2005).

Each face field (ϕ_f) is evaluated using the linear upwind interpolation scheme (LUS) Barth and Jespersen (1989):

$$\phi_f = \phi_P + (\nabla \phi)_P \cdot \mathbf{d}_{fN} \quad (34)$$

Pressure and velocity gradient are evaluated using the linear scheme Blazek (2005). Diffusive terms also are evaluated by the linear scheme without perform orthogonality corrections Blazek (2005), Jasak (1996).

The chemistry data are supplied using the native openFoam reader format OpenCFD (2009). To obtain the source terms into energy and species equations, reaction rates are computed, and species concentrations are updated by solving a stiff system of ordinary differential equation (stiff ODEs) whose dimensions are proportional to the species and reactions of the chemical kinetic model. To solve this stiff ODEs the SIBS method is selected, this method is

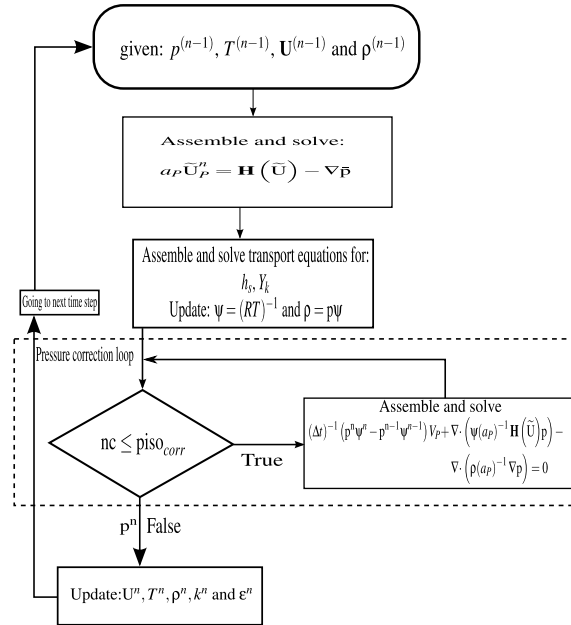


Fig. 2. PISO algorithm flowchart.

based on Richardson extrapolation of the approximated solution. The solver needs to solve ODEs in every time step to determine the chemical species concentrations at the end of the timestep. The Richardson extrapolation of the function ([C]) assumes that as the interval (in our case the computational time step Δt) is split up in to increasing number of sub-steps, the solution will converge to some value ([C(t + Δt)). However, the solver will never apply enough sub-steps to find it. Instead, it will approximate, depending on the solution using large sub-steps. The analytical function used to approximate [C(t + Δt)] is a polynom, and the error function of the method contains only even terms of the step size Bader and Deuffhard (1983) (for more details on solving stiff systems see Hairer and Wanner (2005)).

6. DESCRIPTION OF TEST CASE

The benchmark case selected to test the executable code is the Sandia flame D (Sandia National Laboratories, Ca, USA). This flame D is a piloted non premixed methane and air flame with a main fuel jet Reynolds number (Re_j) at the burner exit of 22400. The pilot is a lean mixture ($\phi = 0.77$) of methane and air and in the calculations it is assumed to behave like an injection of hot burnt gases. The burner exit is positioned approximately 0.15m above the end section of a vertical wind tunnel which provides the air flow.

The burner dimensions are Barlow and Frank (2007):

- Main jet diameter: $d = 0.0072m$
- Pilot annulus outer diameter: $0.0182m$
- Wind tunnel exit section: $0.300m \times 0.300m$

Since the walls of the burner are very thin, no thickness was allocated to walls. The main jet, pilot and air compositions expressed in mass fractions, are given in Tab. 2. Because of the wind tunnel exit dimensions, it is assumed that the simulated flame D develops inside a co-flowing air free jet.

Table 2 Incoming Flow Mass Fractions

	Air	Jet	pilot-bp	pilot-wd	pilot-wdm-jl
N ₂	77	64.73	74.2	73.79	73.72
O ₂	23	19.66	5.4	5.4	5.4
CH ₄	0	15.61	0	0	0
H ₂ O	0	0	9.42	9.42	9.42
CO ₂	0	0	10.98	10.98	10.98
CO	0	0	0	0.407	0.407
H ₂	0	0	0	0	0.0129

6.1 Mesh Generation

The computation domain, discretized using the openFoam utility blockMesh has a length of 0.6m and a radius of 0.15m. The mesh is constructed assuming symmetry about the center line of the main jet, and as Fig. 3 shows it is divided into three blocks.

The first block is defined to include the main jet, the second the pilot region, and the third block covers the air co-flow. An axial stretching

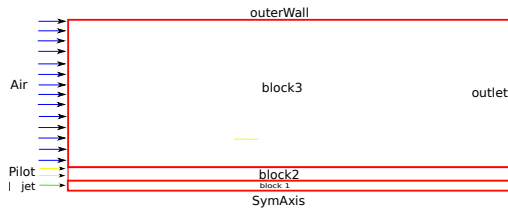


Fig. 3. Computational domain.

factor of 10 is applied, so that cells have minimum length of 0.383mm and maximum length of 3.83mm . The shorter cells are packed close to inlet sections. In the air co-flow the cells are stretched in radial direction with a minimum size of 1.2mm for cells adjacent to block 2. The simulation was run with a mesh arrangement of 40000 cells.

6.2 Boundary and Initial Conditions

In Tab.3 boundary conditions applied to flow variables are listed. The following abbreviations are used: fV for fixed value and zG for zero gradient. To apply boundary conditions in a non-limited by solid surfaces domain, the zero gradient approach is imposed. It has been numerically verified that when the flow is reaching steady state conditions, the assigned outer limit becomes a streamline parallel to the axis of the flow and its velocity approaches the fixed value (0.9m/s) of the air co-flow. This can be interpreted as proof that the free jet approach applied to the domain where the flame D develops, is valid.

Table 3 Boundary conditions⁴

	U_x	p	T	Y	k	ϵ
MJ	49.6	zG	291	fV	Eq. 35	Eq. 36
Air	0.9	zG	294	fV	Eq. 35	Eq. 36
Pilot	11.4	zG	1880	fV	Eq. 35	Eq. 36
OL	zG	zG	zG	zG	zG	zG
Outlet	zG	100615	zG	zG	zG	zG

	I_t	L_t
Main jet	4.569×10^{-2}	5.04×10^{-4}
Air	7.492×10^{-2}	2.10×10^{-2}
Outer Limit	6.030×10^{-2}	7.77×10^{-4}

Starting values for k and ϵ of Main Jet, Air and Pilot are expressed as functions of turbulent intensity (I_t) and characteristic lengths (L_t) respectively. Values for these parameters are computed by using available correlations listed below Wilcox (1998):

$$k = 1.5(uI_t)^2 \quad (35)$$

⁴MJ: Main Jet; OL: Outer Limit

$$\epsilon = 0.1643k^{(3/2)}(L_t)^{-1} \quad (36)$$

Properly determined initial values are important to ensure starting stability and adequate accuracy in solving the conservation equations, and also the effectiveness of the pilot. Inlet conditions for the species equations are set in accordance with flow compositions described in Table. 2. However in the numerical simulation a time dependent technique is used, and initial properties of the flow in the whole computational domain must be defined. They are listed below Barlow and Frank (2007):

$$\left. \begin{aligned} u(0) = 0; T(0) = 300; K p(0) = 94.536 \text{ kPa} \\ Y_{N_2}(0) = 0.77; Y_{O_2}(0) = 0.23; Y_k(0) = 0 \end{aligned} \right\} \quad (37)$$

Note that only for the species O_2 and N_2 mass fractions initial values have been imposed, but not for any other species. This implies that only air is initially present in the computational domain. It should be noted that when the air motion in the computational domain starts, the turbulence properties for the air co-flow are set in terms of the intensity and characteristic length listed in Table 3.

7. RESULTS AND DISCUSSION

The results of openFoam simulations are compared with experimental data of temperature and species. It should be noted that all simplified reaction mechanisms tested are capable of sustaining the diffusive flame started by the pilot. Also note that all results, numerical and experimental, have been plotted in term of the ratio x/r , being x the axial distance and $r = 7.2 \times 10^{-3}\text{m}$, the pilot radius (accordingly with experimental data presented by Barlow and Frank (2007), Barlow (2003)). In Fig. 4, a comparison between experimental and predicted center line temperatures is shown. It can be observed that the one step mechanism has produced acceptable comparisons only in regions where the chemical activity is not the strongest. By assuming that the reaction products are CO_2 and H_2O the total heat of reaction is over predicted. At adiabatic flame temperatures typical of hydrocarbon fuel ($\sim 2000\text{K}$), substantial amounts of CO and H_2 exist in equilibrium with CO_2 and H_2O . The same is true to a lesser extent with other species such as H , O and OH . This equilibrium lowers the total heat of reaction and the

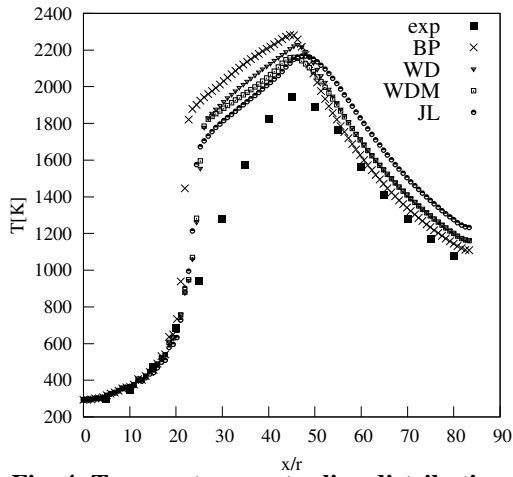


Fig. 4. Temperature center line distribution.

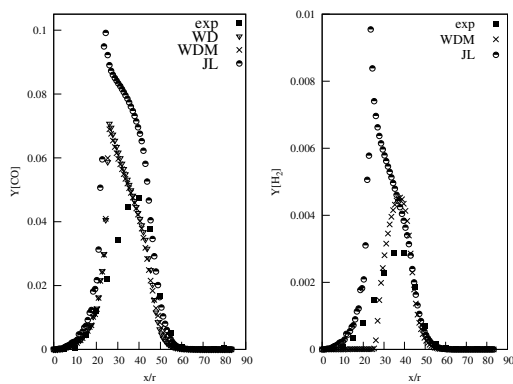


Fig. 5. H₂ and CO center line distributions.

adiabatic flame temperature below values predicted by Bui Pham one step reaction mechanism.

In addition to the fact that the burned gas contains incompletely oxidized species, it is also recognized that typical hydrocarbons burn in a sequential manner, that is, the fuel is partially oxidized to CO and H₂. To account for this effect of incomplete conversion of CH₄ and O₂ reactants to products CO₂ and H₂O, Westbrook and Dryer have introduced the two steps mechanism adding a CO oxidation reaction. This two reactions model is also applied to the methane's flame and temperature results are included in Fig. 4. It can be seen that the addition of the CO - CO₂ equilibrium provides a somewhat better adiabatic flame temperature. Supposedly, further refinements in expressing dissociated effects on burned gas temperature would lead to additional improvements. In this sense, the H₂ oxidation in the Westbrook and Dryer was added, however the flame temperature results did not substantially improved, if compared with the original two steps mechanism.

Comparisons of plotted simulations results us-

ing Jones and Lindstedt four steps mechanism with experiments, have shown no mayor differences when the temperature raises, a small improvement where the heat release should be stronger and some deterioration when the burned gases are diluted by mixing with the cold air coflow. Calculated center line distributions of CH₄, O₂, CO₂ and H₂O mass fractions, are plotted in Fig. 6, and are compared with the Flame "D" experimental data. It is found that CH₄ fuel consumption (Fig. 6(a), is fairly well predicted by all combustion mechanisms proposed. As shown in Fig. 6(b), the O₂ is consumed faster than experimental data and after reaching almost a null value, it start to grow because of mixing with the air coflow. This growing is predicted by all's the combustion mechanisms considered. Regarding CO₂, Fig. 6(c) shows that best approximation to experimental data is obtained with Westbrook and Dryer original two steps mechanism. Results obtained with the four steps reactions of Jones and Lindstedt, Fig. 6(d), have shown tendency to follow the ascending branch of the experimental curve, but a greater divergence in its descending branch. In relation to the behavior of the H₂O simulation, it seems that the one step mechanism provides the best results (Fig. 6(d)). The CO and H₂ mass fractions calculated through the Westbrook and Dryer modified two steps mechanism by adding a H₂ oxidation rate, seem to be best approach to experimental values (Fig. 5).

Simulation times needed to practical reach steady state conditions are derived after applying the $\|L_2\|$ norm to selected variables residuals. Typical results obtained for flow parameters (p, T), species O₂ (reactant) and H₂O (product) in one and four steps combustion mechanisms, are plotted in Fig. 7(a) and Fig. 7(b). It can be concluded that in each of plotted variables a 10^{-6} precision value is achieved with a computation time of not more that one second.

8. CONCLUSIONS

This work has two main proposes. First, to show how an executable code to numerically simulate a rate controlled and turbulent diffusive combustion process, can be built using the set of libraries provided by openFoam. Second, to demonstrate what so good are simulations carried out using the code. It is estimated that the first purpose has been accomplished but the second has been only partially because it produced results that should be conceptualized as not completely satisfactory. Going from one step to two steps, and even to four steps hy-

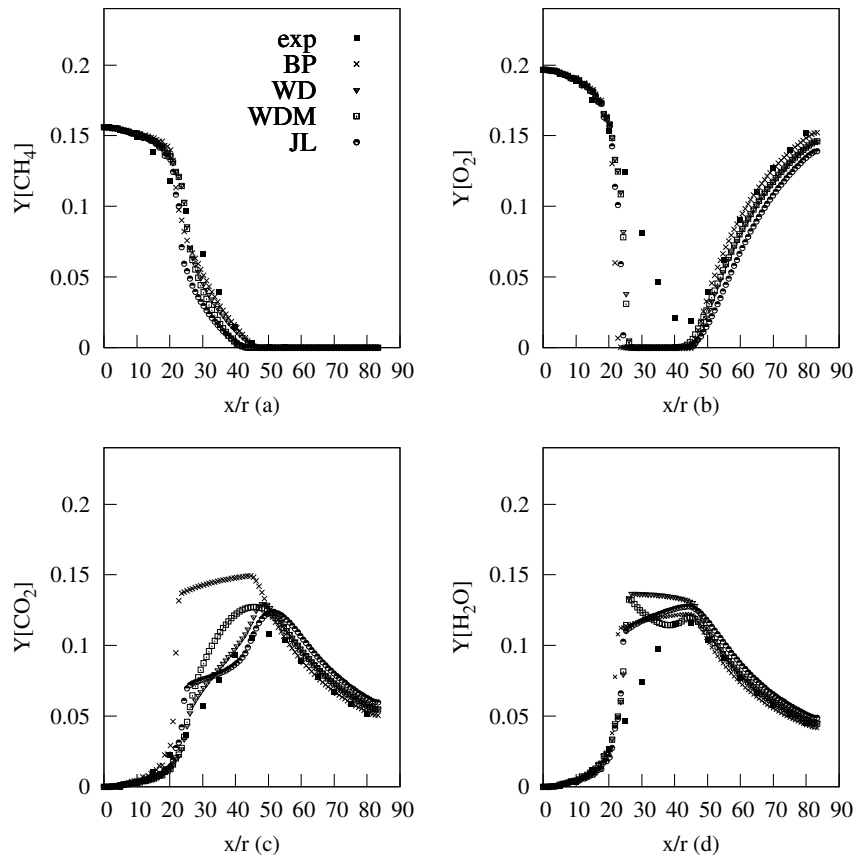


Fig. 6. $\text{CH}_4, \text{O}_2, \text{H}_2\text{O}, \text{CO}_2$ center line distributions.

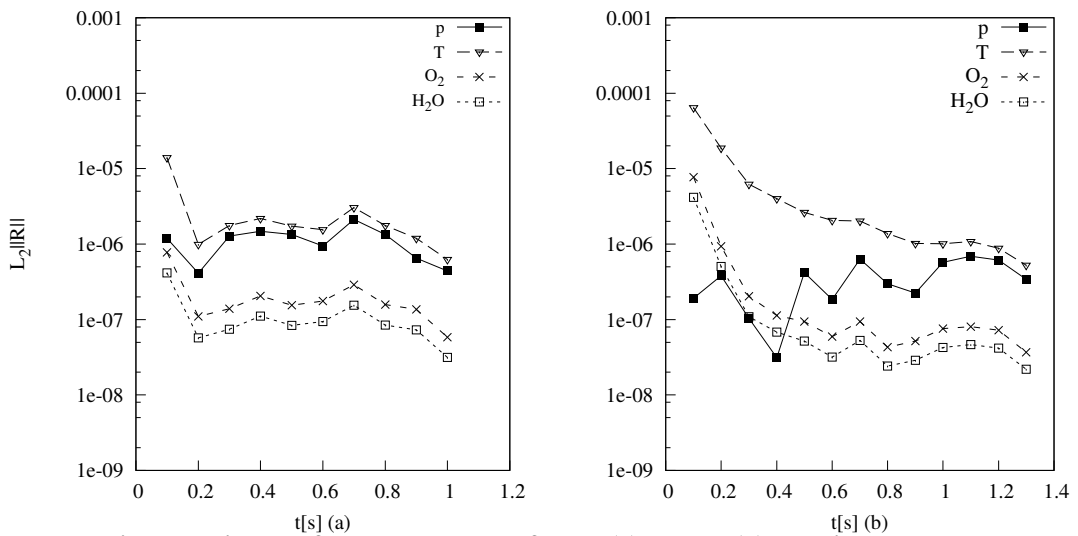


Fig. 7. Residuals of $\text{O}_2, \text{H}_2\text{O}, T$ and p for BP (a) and JL (b) chemical models.

drocarbon combustion mechanisms, carried out simulations do not correctly describe the chemical activity and subsequent heat release, in flow areas where it is most intense. It seems too simplified kinetics models are not capable of describing the recognized sequential manner of the process of hydrocarbons oxidation, given that a detailed combustion mechanism would need around 53 species and 400 elementary reactions. It is to note that losses by radiation are also cause for discrepancies and to take it into account a radiative flux in the energy equation should be incorporated, which has not been done. There are to many unanswered questions about the analytical formulation of radiative flux in diffusion flames.

8.1 Future Work

Marzouk and Huckaby (2010), recommend to work with more complex reaction mechanisms for the oxidation of hydrocarbons fuels in flames, for instance the westbrook1988 model uses 10 species, one global reaction and 21 elementary reversible reactions. It is hope that with more realistic kinetics models, a significant step to reduce differences between experiments and simulations will be given.

ACKNOWLEDGMENTS

To CONICET, MINCYT Crdoba and Aeronautical department of UNC for the financial and facilities support to this research.

REFERENCES

- Andersen, J., C. Rasmussen, T. Giselsson and P. Glarborg (2009). Global combustion mechanisms for use in cfd modeling under oxy-fuel conditions. *Energy & Fuels* 23(3), 1379–1389.
- Bader, G. and P. Deuffhard (1983). A semi-implicit mid-point rule for stiff systems of ordinary differential equations. *Number. Math* 41, 373–398.
- Barlow, R. and J. Frank (2007). Piloted CH_4 /Air flames C, D, E, and F. *Sandia National Laboratories*.
- Barlow, R. A. and J. H. Frank (1998). Effects of turbulence on species mass fractions in methane/air jet flames. In *Symposium (International) on Combustion*, Volume 27, pp. 1087–1095. Elsevier.
- Barlow, R. S. (2003). Sandia TUD Piloted CH_4 -Air Jet Flames. <http://www.sandia.gov/TNF/DataArch/FlameD.html>.
- Barth, T. J. and D. C. Jespersen (1989). The design and application of upwind schemes on unstructured meshes.
- Beaudoin, M. and H. Jasak (2008). Development of a generalized grid interface for turbomachinery simulations with openfoam. In *Open source CFD International conference*, Volume 2.
- Benajes, J., J. Galindo, P. Fajardo and R. Navarro (2014). Development of a segregated compressible flow solver for turbomachinery simulations. *Journal of Applied Fluid Mechanics* 7(4).
- Bird, B. B., W. E. Stewart and E. N. Lightfoot (2007). *Transport phenomena*. John Wiley & Sons.
- Blazek, J. (2005). *Computational Fluid Dynamics: Principles and Applications:(Book with accompanying CD)*. Elsevier.
- Bui-Pham, M. N. (1992). *Studies in structures of laminar hydrocarbon flames*. Ph. D. thesis, Ph.D Thesis,. UCSD.
- Chung, K. L. (2006). *Combustion physics*. Cambridge University Press.
- Concus, P., G. H. Golub and G. Meurant (1985). Block preconditioning for the conjugate gradient method. *SIAM Journal on Scientific and Statistical Computing* 6(1), 220–252.
- Coquel, F., Q. L. Nguyen, M. Postel and Q. H. Tran (2008). *Local time stepping for implicit-explicit methods on time varying grids*. Springer.
- Favre, A. (1969). Statistical equations of turbulent gases. *Problems of hidrodynamics and continuum mechanics*, 231–266.
- Filho, P. M. F., L. da Silva Vieira, , W. D. P. do Nascimento, L. G. Noleto and M. Barcelos (2011). Development of an analysis methodology of aerodynamic profiles applied to design of unmanned aerial vehicles.
- Gutiérrez, L. F., J. P. Tamagno and S. A. Elaskar (2012). High speed flow simulation using openfoam. *Mecánica Computacional, Volume XXXI. Number 16. Aerospatale Technology (A)*.
- Hairer, E. and G. Wanner (2005). Solving ordinary differential equations ii. stiff and differential-algebraic problems.
- Islam, M., F. Decker, E. D. Villiers, A. Jackson, J. Gines, T. Grahs, A. Gitt-Gehrke, I. Font and J. Comas (2009). Application

- of detached-eddy simulation for automotive aerodynamics development. Technical report, SAE Technical Paper.
- Issa, R. I. (1986). Solution of the implicitly discretised fluid flow equations by operator-splitting. *Journal of computational physics* 62(1), 40–65.
- Jasak, H. (1996). *Error Analysis and Estimation for the Finite Volume Method with Applications to Fluid Flows*. Ph. D. thesis, Imperial College of Science, Technology and Medicine.
- Jasak, H. (2007). *Numerical solution algorithms for compressible flows*. Faculty of Mechanical Engineering and Naval Architecture, University of Zagreb, Croatia.
- Jones, W. and J. Launder (1972). The prediction of laminarization with a two-equation model of turbulence. *Int. J. of Heat and Mass Transfer* 15, 301–314.
- Jones, W. P. and R. P. Lindstedt (1988). Global reaction schemes for hydrocarbon combustion. *Combustion and Flame* 73(3), 233–249.
- Kärrholm, F. P. (2008). *Numerical Modelling of Diesel Spray Injection, Turbulence Interaction and Combustion*. Ph. D. thesis, Chalmers University of Technology.
- Kärrholm, F. P., F. Tao and N. Nordin (2008). Three-dimensional simulation of diesel spray ignition and flame lift-off using openfoam and kiva-3v cfd codes. Technical report, SAE Technical Paper.
- Kuo, K. K. (2005). *Principles of Combustion*. John Wiley & Sons, INC.
- Lilleberg, B., D. Christ, I. Ertesvg, R. Kjellerik and R. Kneer (2013). Numerical simulation with an extinction database for use with the eddy dissipation concept for turbulent combustion. *Flow, Turbulence and Combustion* 91(2), 319–346.
- Mangani, L. (2008). Development and validation of an object oriented cfd solver for heat transfer and combustion modeling in turbomachinery application. *Università degli Studi di Firenze, Dipartimento di Energetica*.
- Marinov, M. N., C. K. Westbrook and W. J. Pitz (1996). Detailed and global chemical kinetics model for hydrogen. *Transport phenomena in combustion 1*, 118.
- Marzouk, O. A. and E. D. Huckaby (2010). A comparative study of eight finite-rate chemistry kinetics for CO/h_2 combustion. *Engineering Applications of Computational Fluid Mechanics Vol. 4*(No. 3), 331–356.
- Muntean, S., H. Nilsson and R. F. Susan-Resiga (2009). 3d numerical analysis of the unsteady turbulent swirling flow in a conical diffuser using fluent and openfoam. In *Proceedings of the 3rd IAHR International Meeting of the Workgroup on Cavitation and Dynamic Problems in Hydraulic Machinery and Systems, Brno, Czech Republic, Oct*, pp. 14–16.
- Nooren, P. A., M. Versluis, v. d. M. T. H., R. S. Barlow and J. H. Frank (2000). Raman-rayleigh-lif measurements of temperature and species concentrations in the delft piloted turbulent jet diffusion flame. *Applied Physics B* 71(1), 95–111.
- Nordin, N. P. A. (2001). *Complex Chemistry Modeling of Diesel Spray Combustion*. Ph. D. thesis, Chalmers University of Technology.
- Novella, R., A. García, J. M. Pastor and V. Domenech (2011). The role of detailed chemical kinetics on cfd diesel spray ignition and combustion modelling. *Mathematical and Computer Modelling* 54(7), 1706–1719.
- OpenCFD (2009, 11). *openFoam: User Guide* (1.6 ed.). United Kingdom: OpenCFD Ltd.
- Poinsot, T. and D. Veynante (2005). *Theoretical and Numerical Combustion* (2ed ed.). R. T. Edwards, Inc.
- Singh, A., S. Kumar and K. Nikam (2011). High performance cfd computations for ground vehicle aerodynamics. Technical report, SAE Technical Paper.
- Stull, D. R. and H. Prophet (1971). *JANAF Thermochemical Tables*. 2nd Edition. US National Bureau of Standards. NSRDS-NBS 37.
- Venkatakrisnan, V. and D. J. Mavriplis (1993). Implicit solvers for unstructured meshes. *Journal of computational Physics* 105(1), 83–91.
- Wang, L., L. Zhaohui, C. Sheng and Z. Chuguang (2012). Comparison of different global combustion mechanisms under hot and diluted oxidation conditions. *Combustion Science and Technology* 184(2), 259–276.
- Weller, H., G. Tadmor, H. Jasak and C. Weller (1998). A tensorial approach to

- computational continuum mechanics using object orientated techniques. *Comp. in Phys.* 12(6), 620–630.
- Westbrook, C. K. and F. L. Dryer (1981). Simplified reaction mechanisms for the oxidation of hydrocarbon fuels in flames. *Combustion science and technology* 27(1-2), 31–43.
- Wilcox, D. C. (1998). *Turbulence modeling for CFD*. 2nd Edition. DCW Industries, Inc. - California, US.